Transactions of the Korean Nuclear Society Autumn Meeting
Gyeongju, Korea, October 29-30, 2026

Dynamic Assessment of Feedwater-Flow Proportional–Integral Control for Once-Through Steam Generator Outlet Steam-Temperature Regulation in a Process-Heat High-Temperature Gas-Cooled Reactor

Nayoung Kim [a], Jeong Ik Lee [a*]
[a]*Department of Nuclear and Quantum Engineering Korea Advanced Institute of Science and Technology*
[*]*Corresponding author: jeongiklee@kaist.ac.kr*

**Keywords :* process-heat HTGR, feedwater-heating loss, PI control, once-through steam generator

1. Introduction

Decarbonization of industrial heat requires low-carbon energy systems capable of supplying high-temperature steam under stable thermal conditions. High-temperature gas-cooled reactors (HTGRs) can provide high-grade heat using helium coolant and coated-particle fuel and are therefore applicable to industrial steam production and other high-temperature process applications [1]. Representative HTGR facilities and high-temperature heat utilization concepts are shown in Fig. 1, illustrating the potential integration of nuclear heat with industrial energy systems. When an HTGR is coupled to a once-through steam generator (OTSG), variations in secondary-side conditions can directly affect the delivered steam temperature. Feedwater-flow regulation provides a means of compensating for these variations during process-heat operation.

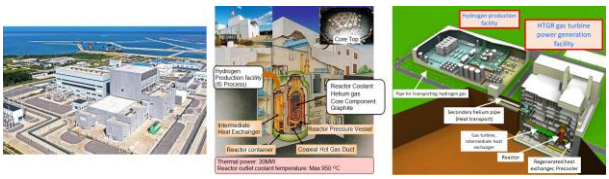


Fig. 1 Representative HTGR facility and high-temperature heat utilization concepts. (a) HTGR facility, (b) reactor and heat-transfer configuration, and (c) HTGR integration with hydrogen production and power generation.

Previous HTGR control studies have investigated the regulation of reactor power and steam conditions using primary- and secondary-side actuators. Dong developed a nonlinear coordinated control system for a nuclear steam supply system (NSSS) based on a modular high-temperature gas-cooled reactor (MHTGR) using control-rod motion, helium flow, and feedwater flow [2]. Jiang and Dong subsequently applied dynamic matrix control to regulate major NSSS variables, including the main steam condition [3]. Wu et al. evaluated load-following control for an integrated HTR-PM model including the reactor, OTSG, turbine, and feedwater-heating system [4]. A previous quasi-steady assessment of the 90 MWth process-heat HTGR considered in this study showed that variations in feedwater conditions affect the coupled primary- and secondary-side responses [7].

Feedwater temperature is particularly relevant because it directly determines the inlet enthalpy of an OTSG. Wu et al. showed that the transient response of a helical-coil OTSG is sensitive to variations in feedwater temperature and flow rate [5]. Loss of feedwater heating is explicitly identified as a Service Level B off-normal event in the MHTGR Plant Design Duty Cycle (PDDC) [6]. For limited main-loop overcooling, including loss of deaerator heating, the PDDC states that the nuclear-island control system should maintain steam delivery at rated conditions without incurring a protective-system trip. However, the PDDC does not prescribe a numerical allowable steam-temperature deviation or settling time for this event. In an HTR-PM full-scale simulator study, Dong et al. evaluated sudden bypass of a high-pressure feedwater heater at full reactor power and showed that the resulting feedwater-temperature reduction affected the live steam temperature, reactor inlet helium temperature, reactor power, and main steam pressure [8]. The cited HTGR control studies mainly addressed coordinated or plant-level regulation involving multiple system variables. The present study isolates the secondary-side control response by maintaining the reactor at nominal full power and imposing loss of feedwater heating as a feedwater-enthalpy disturbance. Feedwater flow is then used as the sole manipulated variable to examine whether the OTSG outlet steam temperature can be recovered without additional reactor-power control.

Accordingly, this study evaluates feedwater-flow proportional–integral (PI) control for OTSG steam-temperature regulation during loss of feedwater heating in a process-heat HTGR. The reactor is maintained at nominal full power, while the OTSG outlet steam temperature and feedwater flow are selected as the controlled and manipulated variables, respectively. GAMMA+ transient calculations are used to evaluate steam-temperature recovery and the corresponding feedwater flow response. The secondary-side response is further examined to distinguish the observed temperature dynamics from gain-specific controller oscillation.

2. Methods and Results

In this section, the feedwater-heating loss is defined from the HTGR heat balance and implemented in GAMMA+ with PI control. Performance is assessed using temperature deviation, settling time, and feedwater-flow demand.

2.1 System Configuration and Feedwater-heating loss Scenario

Fig. 2 presents the HTGR heat-transfer system, the physical origin of the feedwater-heating loss, and the associated steam-temperature control loop. Thermal energy generated in the reactor core is transferred by the primary helium coolant to the helical-coil once-through steam generator. Pressurized feedwater passes through the economizing, evaporation, and superheating regions of the OTSG and is discharged as superheated process steam. A small fraction of the generated steam is diverted to the feedwater heater to increase the feedwater enthalpy before entering the OTSG.

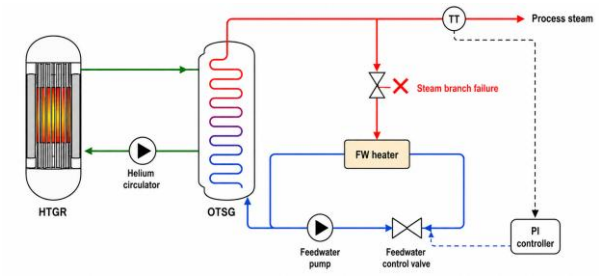


Fig. 2 Schematic of the process-heat HTGR system and feedwater-flow PI control under loss of feedwater heating.

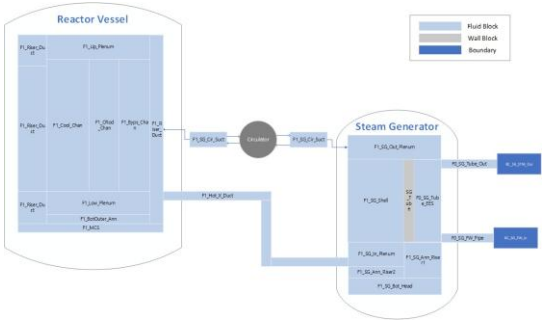


Fig. 3 Simplified nodalization of the HTGR–OTSG system for feedwater-flow PI control.

The nominal operating conditions and feedwater-heating parameters derived from the reference-system heat balance are summarized in Table I.

The initiating event considered in this study is the complete loss of the heating-steam branch. Physically, the event represents complete isolation of the heating-steam branch and the corresponding loss of feedwater-heating duty. This represents a loss of feedwater heating rather than a loss of feedwater flow. Feedwater circulation is maintained while the thermal contribution of the feedwater heater is removed. The event definition is consistent with the loss-of-feedwater-heating event identified in the MHTGR Plant Design Duty Cycle [6].

The feedwater heater and heating-steam branches are included in Fig. 2 to define the physical origin of the disturbance but are not explicitly represented in the GAMMA+ computational domain. The loss of heating duty was therefore converted into an equivalent OTSG inlet boundary condition. Removal of the nominal feedwater-heating duty corresponds to an approximately 15 °C reduction in the OTSG inlet feedwater temperature based on the reference-system heat balance.

The disturbance was implemented as a step change in the OTSG inlet feedwater temperature. A similar treatment was adopted in the HTR-PM full-scale simulator study by Dong et al. [8], where sudden bypass of a high-pressure feedwater heater at full reactor power was represented by an approximately 30 °C step decrease in the corresponding NSSS feedwater temperature. The reduction used in the present study was independently derived from the reference-system heat balance after removal of the nominal feedwater-heating duty. The HTR-PM study was used only as precedent for representing a rapid feedwater-heating loss as a step change in feedwater temperature.

The heating-steam flow isolated from the feedwater heater was not redistributed to the process-steam line in the computational model. Reactor thermal power and the external process-steam boundary condition were maintained at their nominal values so that the transient response primarily reflected the reduction in OTSG inlet feedwater enthalpy and the subsequent action of the feedwater-flow controller.

Table I. Conditions and feedwater-heating loss input

Parameter	Condition
Reactor power	100%
Steam-temperature set point	Stabilized pre-disturbance value
Initial feedwater flow rate	Nominal value
Heating-steam branch	Fully isolated
Feedwater-heating duty	Removed
OTSG inlet feedwater temperature	Approximately 15 °C step reduction

2.2 PI control strategy and simulation procedure

The OTSG outlet steam temperature was selected as the controlled variable and the feedwater mass flow rate was selected as the manipulated variable. The steam-temperature set point was defined as the stabilized pre-disturbance value obtained from the nominal full-power calculation. The control error was defined as

$$e(t) = T_{steam,out}(t) - T_{set}$$

where $T_{steam,out}$ and T_{set} denote the measured and target steam outlet temperatures, respectively. The feedwater-flow command was calculated as

$$\dot{m}_{FW}(t) = \dot{m}_{FW,0} + K_p e(t) + K_i \int_0^t e(\tau) d\tau$$

where $\dot{m}_{FW,0}$ is the nominal feedwater flow rate, and K_p and K_i are the proportional and integral gains, respectively. With temperature error expressed in K and feedwater flow in kg/s, K_p and K_i have units of $\mathrm{kg/s \cdot K}$ and $\mathrm{kg/s^2 \cdot K}$, respectively. With the adopted error definition, a decrease in the OTSG outlet steam temperature produces a reduction in the commanded feedwater flow. The decrease in feedwater flow increases the thermal energy transferred per unit secondary-side mass and thereby provides reverse-acting compensation for the reduction in feedwater inlet enthalpy.

The calculated PI command was directly applied to the secondary-side feedwater-flow boundary without actuator dynamics, output saturation, or anti-windup treatment. Accordingly, the present response represents controller behavior under idealized actuation rather than a plant-qualified control system. Application-level suitability would require further evaluation of actuator dynamics and rate limits, output saturation, transport and measurement delays, anti-windup treatment, and relevant protection-system setpoints. The transient calculation was initialized from the stabilized nominal full-power condition. The corresponding pre-disturbance steam outlet temperature was used as the controller reference, and PI control was activated at disturbance initiation.

The controller gains were evaluated sequentially. The integral gain was first varied while the proportional gain was fixed. The integral gain selected from this assessment was then retained while the proportional gain was varied.

The control response was evaluated using the maximum steam-temperature deviation, settling time, feedwater peak-to-peak excursion, and attenuation of successive transient excursions. Settling time was defined as the elapsed time after disturbance initiation until the OTSG outlet steam temperature entered the ±0.1 °C band around the set point and remained within this band. The ±0.1 °C band was introduced solely as an analysis-defined metric for quantifying controller settling and does not represent a plant acceptance limit. The MHTGR PDDC does not specify a numerical steam-temperature tolerance or settling-time requirement for loss of feedwater heating [6]. Therefore, plant-level relevance in the present study is assessed by whether the controller restores the outlet steam temperature toward the rated pre-disturbance condition with a bounded and damped response. Service Level B component qualification, which requires components to withstand the specified event loadings without damage requiring repair, is outside the scope of the present thermal-hydraulic control analysis.

The feedwater peak-to-peak excursion quantified the flow variation, while successive excursion attenuation was used to distinguish damped responses from persistent oscillations.

2.3 PI gain sensitivity and gain selection

Fig. 4 shows the sensitivity of the steam-temperature and feedwater-flow responses to the PI gains. Increasing the integral gain accelerated the decay of the residual temperature error, whereas the initial temperature excursion changed to a lesser extent. The higher integral-gain cases showed similar recovery responses. For presentation, the PI gains in Fig. 4 were normalized by the selected gain values, such that a normalized value of unity corresponds to the gains used in the subsequent transient analysis.

Increasing K_p reduced the initial steam-temperature excursion. The maximum absolute temperature deviation decreased from approximately 3.1 °C to 1.7 °C over the investigated gain range. At higher K_p, the peak deviation continued to decrease, while the settling time increased. The corresponding feedwater-flow responses remained within a similar range.

All investigated cases remained bounded, and successive temperature excursions decreased after the initial overshoot and undershoot. No sustained oscillation was observed. Based on the temperature excursion, settling behavior, and feedwater-flow response shown in Fig. 4, the selected PI gains were used for the subsequent transient analysis.

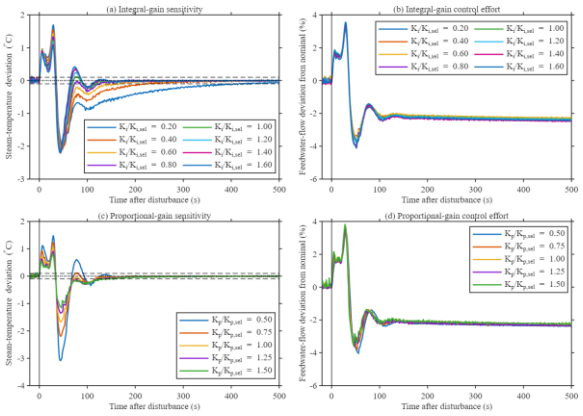


Fig. 4 PI-gain sensitivity of the steam-temperature and feedwater-flow responses

2.4 Controlled response to loss of feedwater heating

Fig. presents the controlled response obtained with the selected PI gains. An approximately 15 °C step reduction in the OTSG inlet feedwater-temperature boundary condition was imposed at disturbance initiation, as shown in Fig. 5.

The OTSG outlet steam temperature showed an initial non-monotonic response. The deviation first reached approximately +1.0 °C and subsequently decreased to approximately −1.7 °C. The outlet temperature entered and remained within the analysis-defined ±0.1 °C settling band after approximately 120 s. Successive temperature excursions decreased with time, and no sustained oscillation was observed. The 120 s value

therefore represents the settling time of the simulated controller rather than an externally imposed plant recovery-time requirement. The response restored the outlet steam temperature toward the pre-disturbance rated condition, which is qualitatively consistent with the PDDC functional expectation for limited overcooling [6]. However, because protection-system setpoints and component structural loadings were not evaluated, this result does not demonstrate full Service Level B qualification.

The feedwater flow initially increased to approximately 3.4% above its nominal value and subsequently decreased to approximately 3.5% below nominal before approaching a quasi-steady condition. The applied feedwater flow followed the PI command throughout the transient. No appreciable deviation between the commanded and applied flow was observed during the principal steam-temperature excursion.

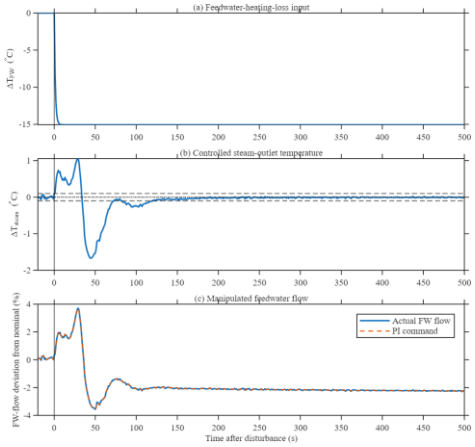


Fig. 5 Controlled response to loss of feedwater heating

The secondary-side response was further examined to characterize the initial steam-temperature reversal. The net secondary-side enthalpy flow was calculated as

$$\dot{H}_{sec} = \dot{m}_{steam} h_{steam,out} - \dot{m}_{FW} h_{FW,in}$$

where the instantaneous steam and feedwater mass flow rates were used independently. The responses in Fig. 6 are expressed as deviations from their pre-disturbance reference values, with a common mass-flow reference used for the feedwater and steam flows. The calculated $\dot{H}_{sec}$ increased rapidly after disturbance initiation, while a transient difference developed between the feedwater and steam mass flow rates.

During the early transient, the feedwater mass flow exceeded the steam mass flow, producing a temporary increase in secondary-side fluid inventory. The steam mass flow subsequently exceeded the feedwater mass flow, corresponding to a reduction of the accumulated inventory. This flow reversal occurred over the same time interval as the principal turning points of the steam-temperature response.

The steam-temperature turning points occurred over the same time interval as the secondary-side mass-flow redistribution. Similar turning points were observed for different PI gains in Fig. 4, while gain variation changed the magnitude and attenuation of the response. The repeated occurrence of the turning behavior together with the transient feedwater-to-steam flow imbalance supports an interpretation involving secondary-side inventory redistribution and thermal transport within the OTSG.

Axial boiling-boundary motion and local void-fraction evolution were not examined in the present analysis. The contribution of boiling-front motion to the observed temperature response was therefore not separately quantified. Table II summarizes the performance of the selected PI controller, including the steam-temperature excursion, settling time, feedwater-flow range, and damping characteristics.

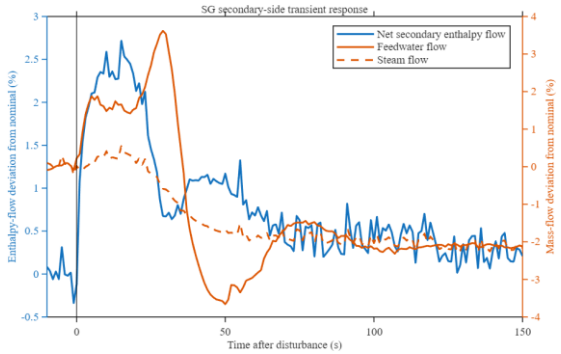


Fig. 6 Secondary-side thermal-hydraulic response during loss of feedwater heating

Table II. Summary of the PI-controlled response

Performance metric	Result
Maximum positive temperature deviation	+1.0℃
Maximum negative temperature deviation	-1.7℃
Settling band (analysis definition)	±0.1℃
Settling time	120s
Maximum feedwater-flow deviation	+3.4% of nominal
Minimum feedwater flow deviation	−3.5% of nominal
Feedwater flow peak-to-peak excursion	6.9% of nominal

3. Conclusions

This study assessed the dynamic capability of feedwater-flow PI control to restore the OTSG outlet steam temperature following a complete loss of feedwater heating while reactor power remained at nominal full power. The feedwater-heating loss was represented by an approximately 15 °C reduction in the OTSG inlet feedwater temperature derived from the reference-system heat balance after removal of the nominal feedwater-heating duty. The selected controller limited the steam-temperature deviation to approximately +1.0/−1.7 °C and entered the analysis-

defined ±0.1 °C settling band after approximately 120 s without sustained oscillation. The PDDC identifies loss of feedwater heating as a Service Level B event and expects rated steam delivery to be maintained for limited overcooling [6]; the simulated temperature recovery is qualitatively consistent with this functional objective. However, the ±0.1 °C band and 120 s settling time are not PDDC acceptance limits, and the present model does not establish plant qualification or Service Level B structural compliance because actuator dynamics, protection-system setpoints, and component stress were not evaluated. The initial non-monotonic response coincided with a transient imbalance between the feedwater and steam mass flow rates and the associated redistribution of secondary-side fluid inventory. Similar turning behavior over the investigated PI-gain range supports an interpretation involving both controller response and OTSG secondary-side thermal-hydraulic dynamics.

ACKNOWLEDGEMENT

This work was supported by the National Research Foundation of Korea (NRF) grant funded by the Korea government (MSIT) (No. RS-2024-00457356).

REFERENCES

[1] OECD Nuclear Energy Agency, *High-temperature Gas-cooled Reactors and Industrial Heat Applications*, OECD Publishing, 2022.
[2] Z. Dong, “Nonlinear coordinated control for MHTGR-based nuclear steam supply systems,” *IEEE Transactions on Nuclear Science*, Vol. 61, No. 5, pp. 2643–2656, 2014.
[3] D. Jiang and Z. Dong, “Practical dynamic matrix control of MHTGR-based nuclear steam supply systems,” *Energy*, Vol. 185, pp. 695–707, 2019.
[4] S. Wu, X. Ma, J. Liu, J. Wan, P. Wang, and G. H. Su, “A load following control strategy for Chinese Modular High-Temperature Gas-Cooled Reactor HTR-PM,” *Energy*, Vol. 263, 125459, 2023.
[5] S. Wu, Z. Li, P. Wang, G. H. Su, and J. Wan, “A three-region movable-boundary helical coil once-through steam generator model for dynamic simulation and controller design,” *Nuclear Engineering and Technology*, Vol. 55, No. 2, pp. 460–474, 2023.
[6] T. Chan, *Modular High Temperature Gas-Cooled Reactor Plant Design Duty Cycle, Revision 3*, DOE/HTGR-86029-Rev.3, 1989.
[7] N. Kim and J. I. Lee, “Preliminary Feasibility Assessment of PRDBE-Based Control for Process Heat HTGRs,” *Transactions of the Korean Nuclear Society Spring Meeting*, Jeju, Korea, 2026.
[8] Z. Dong, Y. Pan, X. Huang, Y. Dong, and Z. Zhang, “Coordinated control system design and verification of HTR-PM plant,” *Nuclear Engineering and Design*, Vol. 329, pp. 25–33, 2018.